Measurement of the properties of the η' and search for other resonances in $\gamma\gamma \to \eta\pi^0\pi^0$

D. Antreasyan,[θ] H. W. Bartels,[δ] D. Besset,[κ] Ch. Bieler,[η] J. K. Bienlein,[δ] A. Bizzeti,[ζ] E. D. Bloom,[λ] I. Brock,[β] K. Brockmüller,[δ] R. Cabenda,[κ] A. Cartacci,[ζ] M. Cavalli-Sforza,[κ,(a)] R. Clare,[λ,(b)] G. Conforto,[ζ] S. Cooper,[λ,(b)] R. Cowan,[κ,(b)] D. Coyne,[κ,(a)] G. Drews,[δ] C. Edwards,[α] A. Engler,[β] K. H. Fairfield,[λ] G. Folger,[ε,(c)] A. Fridman,[λ,(d)] J. Gaiser,[λ] D. Gelphman,[λ] G. Glaser,[ε] G. Godfrey,[λ] F. H. Heimlich,[η,ζ] R. Hofstadter,[λ] J. Irion,[θ] Z. Jakubowski,[γ] K. Karch,[μ] S. Keh,[μ,(e)] H. Kilian,[μ] I. Kirkbride,[λ] T. Kloiber,[δ] M. Kobel,[ε] W. Koch,[δ] A. C. König,[ι] K. Königsmann,[μ] R. W. Kraemer,[β] S. Krüger,[η] G. Landi,[ζ] R. Lee,[λ] S. Leffler,[λ] R. Lekebusch,[η] A. M. Litke,[λ,(a)] W. Lockman,[λ,(a)] S. Lowe,[λ] B. Lurz,[ε] D. Marlow,[β,κ] H. Marsiske,[δ] W. Maschmann,[η] T. Matsui,[λ,(f)] P. McBride,[θ] F. Messing,[β] W. J. Metzger,[ι] H. Meyer,[δ] B. Monteleoni,[ζ] R. Nernst,[η] B. Niczyporuk,[λ,(g)] G. Nowak,[γ] C. Peck,[α] P. G. Pelfer,[ζ] B. Pollock,[λ] F. C. Porter,[α] D. Prindle,[β,(h)] P. Ratoff,[α,(i)] B. Renger,[β] C. Rippich,[β] M. Scheer,[μ] P. Schmitt,[μ,θ] J. Schotanus,[ι] A. Schwarz,[λ,(a)] F. Selonke,[δ] D. Sievers,[η] T. Skwarnicki,[δ,(g)] V. Stock,[η] K. Strauch,[θ] U. Strohbusch,[η] J. Tompkins,[λ,(j)] H. J. Trost,[δ,(k)] R. T. Van de Walle,[ι] H. Vogel,[β] A. Voigt,[δ] U. Volland,[ε] K. Wachs,[δ] K. Wacker,[λ,(l)] W. Walk,[ι,(m)] H. Wegener,[ε] D. Williams,[θ,(a)] and P. Zschorsch[δ]

[α]*California Institute of Technology, Pasadena, California 91125*
[β]*Carnegie-Mellon University, Pittsburgh, Pennsylvania 15213*
[γ]*Cracow Institute of Nuclear Physics, Cracow, Poland*
[δ]*Deutsches Elektronen Synchrotron DESY, Hamburg, West Germany*
[ε]*Universität Erlangen-Nürnberg, Erlangen, West Germany*
[ζ]*Istituto Nazionale di Fisica Nucleare and University of Firenze, Firenze, Italy*
[η]*Institut für Experimentalphysik I, Universität Hamburg, Hamburg, West Germany*
[θ]*Harvard University, Cambridge, Massachusetts 02138*
[ι]*University of Nijmegen and Nationaal Instituut voor Kernfysica en Hoge-Energiefysica-Nijmegen, Nijmegen, The Netherlands*
[κ]*Princeton University, Princeton, New Jersey 08544*
[λ]*Department of Physics, High Energy Physics Laboratory and Stanford Linear Accelerator Center, Stanford University, Stanford, California 94305*
[μ]*Universität Würzburg, Würzburg, West Germany*
(The Crystal Ball Collaboration)
(Received 17 June 1987)

The reaction $e^+e^- \to e^+e^-\eta\pi^0\pi^0$ has been observed with the Crystal Ball detector at the DORIS II storage ring at DESY. The $\eta\pi^0\pi^0$ mass spectrum is dominated by the η', and the two-photon width $\Gamma_{\eta' \to \gamma\gamma}$ is determined to be $4.6 \pm 0.4 \pm 0.6$ keV. Limits on $\Gamma_{X \to \gamma\gamma} \times B_{X \to \eta\pi\pi}$ are given for other possible states.

I. INTRODUCTION

The partial widths of mesons to two photons give information on their quark content. The degree of mixing between SU(3) octet and singlet of the ground-state pseudoscalar nonet affects the relative two-photon widths of the π^0, η, and η' mesons, as would possible mixing with a glueball. Radially excited pseudoscalar mesons could participate in the mixing, and might also be seen directly in two-photon collisions. The $\gamma\gamma \to \eta\pi^0\pi^0$ reaction is well suited to searching for new $I=0$ pseudoscalars since $\eta\pi^0\pi^0$ is limited to $I=0$ or 2, and $J^P=0^-$ is achieved without any orbital angular momentum.

In this paper we present an analysis of the reaction $e^+e^- \to e^+e^-\eta\pi^0\pi^0$, with $\eta \to \gamma\gamma$. The outgoing e^+ and e^- scatter at very small angles and are not observed (no tag); thus the observed final state consists of six photons. The $\eta\pi^0\pi^0$ mass spectrum is dominated by the η', and is used to extract its two-photon width $\Gamma_{\eta' \to \gamma\gamma}$. Since the η and π^0 are narrow spinless particles, the complications inherent in measuring the η' via its $\gamma\rho$ decay are avoided. Upper limits are set on heavier mesons decaying to $\eta\pi^0\pi^0$.

The data were taken using the Crystal Ball detector at the DORIS II e^+e^- storage at DESY and represent an accumulated luminosity of 131 pb^{-1}. Most of the running was on the various resonances of the Υ system with an average center-of-mass energy of 10 GeV.

II. DETECTOR AND TRIGGER

The Crystal Ball detector,[1] shown in Fig. 1, is a nonmagnetic calorimeter designed to measure the energies and directions of electromagnetically interacting particles. The main detector is a highly segmented spherical shell of NaI(Tl) which covers 93% of the total solid an-

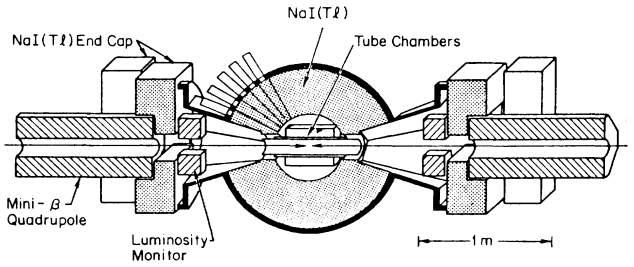

FIG. 1. The Crystal Ball detector.

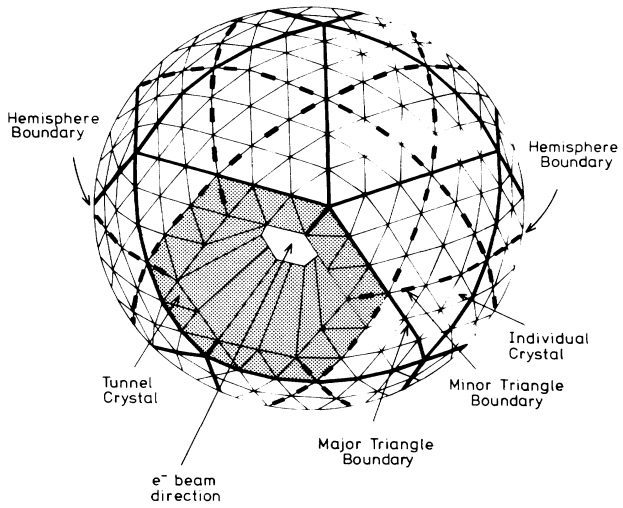

FIG. 2. The organization of the individual crystals into major and minor triangles, and into top and bottom hemispheres. The shaded area is the layer of "tunnel crystals" next to the beam.

gle. It contains 672 optically isolated crystals, each viewed by a phototube. Each crystal is a truncated triangular pyramid 16 radiation lengths deep pointing towards the interaction point. The segmentation of the spherical shell is based on an icosahedron, as shown in Fig. 2. Each of the 20 triangular faces, referred to as "major triangles," is subdivided into four "minor triangles" each consisting of nine individual crystals. A complete 4π ball would contain 720 crystals; to allow entry and exit of the beams, 24 crystals from each of two diametrically opposed regions are omitted. The 30 crystals immediately surrounding each beam hole are called the "tunnel crystals." The remaining crystals, covering 85% of 4π, make up the "main ball." NaI(Tl) end caps cover an additional 5% of 4π, but are not used in the analysis presented here.

The measured energy resolution for electromagnetically showering particles is $\sigma_E/E=(2.7\pm0.2)\%/\sqrt[4]{E}$ (E in GeV), with the energy shared among a symmetric cluster of 13 neighboring crystals. A photon deposits on average 70% of its energy in the central crystal, and about 2% is outside the cluster of 13. This pattern of lateral energy deposition is useful in identifying electromagnetically showering particles. Using the distribution of energy within the cluster, we determine the directions of showering particles to an accuracy ranging from about 3° for the polar angle of a 70-MeV photon to about 2° at 500 MeV. The NaI(Tl) energy scale is set for each ~ 3 pb^{-1} of accumulated data using large-angle Bhabha-scattering events. We use our studies of the $\Upsilon(2S)\to\pi^0\pi^0\Upsilon(1S)$ channel to correct our calibration at lower energies by a one-parameter nonlinear expression,[2] which gives a correction of $+5\%$ at 100 MeV.

Charged particles are detected in a set of cylindrical proportional tube chambers which surround the beam pipe. There were originally three double-layered chambers filled with "magic gas." They have been replaced in stages by a set of four double layers filled with a (79-20-1)% Ar-CO_2-methane mixture. The beam pipe has a thickness corresponding to 0.017 radiation lengths (r.l.). Each double-layer chamber adds 0.010 r.l. in the old and 0.017 r.l. in the new configuration. In the analysis presented here, we are interested in all-neutral final states, and use the chamber information to reject events with charged tracks. Although the chambers can be used for tracking, we find it sufficient here to simply count chamber "hits" with pulse-height discriminators which are also used in the trigger. We use the hits in the third chamber, which is at a radius of 14.5 cm (11 cm) and covers 78% (87%) of 4π in the old (new) configuration.

The triggers are based on fast analog sums of the energy deposited in the main ball, its top and bottom hemispheres, and each of its major triangles. These are subjected to various discriminator thresholds. The tunnel crystals are excluded from these sums, giving an effective trigger solid angle of 85% of 4π. For use in vetoing beam gas and other events originating far from the in-

TABLE I. Triggers.

Trigger name	Min. E in main ball (MeV)	Max. E in tunnels (MeV)	Chamber veto?	Additional requirements
2 hemisphere	800	30	No	>180 MeV in top, bottom
6 hemisphere	860	No limit	Yes	≥ 1 major with >150 MeV in each of 6 hemispheres
Multiplicity	450	30	Yes	≥ 3 majors with >110 MeV
Combination	800	65	No	≥ 1 major with >60 meV in each of 6 hemispheres and ≥ 3 majors with >110 MeV

TABLE II. List of run periods with luminosity, triggers, efficiencies, fitted number of observed η's, and resulting product of η' two-photon width and decay branching ratio. The errors quoted are statistical only.

Run period	1	2	3	4	5	6
Luminosity (pb^{-1})	32.2	32.2	20.0	13.5	19.0	14.2
$\langle E_{c.m.} \rangle$ (GeV)	10.02	10.02	9.46	10.6	10.6	10.6
$\bar{\sigma}_{\eta'}$ (nb)	0.164	0.164	0.156	0.172	0.172	0.172
Triggers						
2 hemisphere	×	×	×	×	×	×
6 hemisphere		×	×	×		
Multiplicity		×				
Combined					×	×
ϵ_{trig}	0.69	0.86	0.84	0.84	0.91	0.94
ϵ_{neut}	0.77±0.02	0.77±0.02	0.74±0.03	0.78±0.03	0.82±0.09	0.79±0.03
Total efficiency ϵ	0.0180	0.0222	0.0207	0.0218	0.0248	0.0247
$N_{\eta'}$	37.5±6.3	49.1±7.4	24.3±5.0	16.5±4.1	34.7±5.9	24.8±5.1
$B_{\eta'\to 6\gamma} \times \Gamma_{\eta'\to\gamma\gamma}$ (keV)	0.39±0.07	0.42±0.07	0.38±0.08	0.33±0.08	0.43±0.09	0.41±0.09

teraction point, the energies in the tunnel crystals are summed and discriminated separately, as are the pulse heights in the chambers. The final trigger decisions are based on various logical combinations of the discriminator outputs, all of which are recorded on tape for each triggered event. Thus by examining events which satisfied more than one trigger, the separate thresholds and efficiencies can be determined. After measuring the hardware thresholds in this way, we set sharp software thresholds safely above them (below for vetoes). Events used in the analysis presented here are required to satisfy these software thresholds, which are given in the following trigger descriptions.

Designing a trigger for a no-tag $\gamma\gamma$ experiment is difficult since the energy deposited in the detector is small compared to the beam energy. We use a combination of four different triggers to optimize the η' efficiency while keeping the backgrounds low and accommodating to changing conditions. Three of the triggers use a technique of dividing the ball into hemispheres with planes containing the beam axis, and requiring that each hemisphere contain a minimum energy. Since the outgoing leptons of our process are usually scattered at very small angles, the detected event has nearly balanced transverse momentum (p_t), and will thus satisfy the above requirement; whereas backgrounds, e.g., from off-axis electrons, tend to deposit energy in only one hemisphere. A veto on energy deposited in the tunnel crystals is effective in reducing backgrounds which do not come from the interaction point, but also reduces the effective solid angle of the detector. Events with charged particles can be eliminated by vetoing events which have a hit in the third chamber. The four triggers used in this analysis are various combinations of the above requirements. They are summarized in Table I and are described in detail below.

(i) The 2-hemisphere trigger requires a total energy deposition of >800 MeV in the main ball and >180 MeV in its top and in its bottom hemisphere. This trigger is vetoed by a total of >30 MeV in the tunnel crystals.

(ii) The 6-hemisphere trigger requires >860 MeV in the main ball. The p_t balance requirement is strengthened over that of the first trigger by dividing the ball into six hemispheres with three different planes containing the beam axis, and requiring that each hemisphere contain $\geq$one major triangle with >150 MeV. The trigger is vetoed by a hit in the third chamber.

(iii) The multiplicity trigger requires >450 MeV in the main ball and a multiplicity of $\geq$three major triangles with >110 MeV each. It is vetoed by a hit in the third chamber, or by >30 MeV in the tunnel crystals.

(iv) The combined trigger requires >800 MeV in the main ball, >60 MeV in each of the hemispheres of the 6-hemisphere trigger, and $\geq$three major triangles with >110 MeV each. It is vetoed by >65 MeV in the tunnel crystals.

The 2-hemisphere trigger was installed during the collection of the entire data sample. The Monte Carlo studies described in Sec. IV show that it is 69% efficient for η' events passing all cuts except the trigger requirement. Adding the 6-hemisphere and multiplicity triggers brought the efficiency up to about 85%; they were installed for 66 and 32 pb^{-1}, respectively. During the 33 pb^{-1} that the combined trigger was installed the efficiency was over 90%. The triggers installed for each run period and the resulting efficiencies are summarized in Table II.

III. SELECTION CRITERIA

All events used in this analysis are first passed through a filter program designed to select events produced by two-photon collisions by requiring total deposited energy $E_{tot} < 5$ GeV and net transverse momentum $|\sum \mathbf{p}_t| < 200$ MeV/c. The $|\sum \mathbf{p}_t|$ is calculated by assigning a vector $\mathbf{p}$ to each crystal in the main ball and tunnels with magnitude equal to the energy seen in that crystal.

The events must satisfy a software trigger filter with thresholds set higher than those in the hardware, as described in the previous section. This eliminates effects from small variations in the trigger thresholds, and also facilitates efficiency calculations. All-neutral events are

selected by requiring that the chamber-3 discriminator was not set. This requirement is the same as that used in the 6-hemisphere and multiplicity triggers described above. Thus, a uniform neutrality cut is used, regardless of whether it is applied at the trigger level, or via this cut.

After this preselection the following criteria are used to select six-photon final states.

(i) There must be exactly six clusters of energy in the ball of >20 MeV each. They are the photon candidates.

(ii) The six photons must each have $|\cos\theta|<0.9$, where θ is the angle between the photon direction and the beam axis.

(iii) The lateral energy deposition of each photon candidate must be consistent with that expected from an electromagnetic shower.

Candidate $\eta\pi^0\pi^0$ events are searched for by grouping the six photons in pairs. There are 15 different ways of combining six photons into three pairs. The two-photon invariant mass ($M_{\gamma\gamma}$) for all photon pairs is shown in Fig. 3. Events with at least one pair within ± 60 MeV of the η mass are selected. For these events we plot $M^{(1)}_{\gamma\gamma}$ vs $M^{(2)}_{\gamma\gamma}$ for the remaining four photons. This is shown in Fig. 4, where there are three entries for each η candidate. There is a clear clustering of events containing two π^0's. We accept events with

$$(M^{(1)}_{\gamma\gamma}-M_{\pi^0})^2+(M^{(2)}_{\gamma\gamma}-M_{\pi^0})^2<1200\ (\mathrm{MeV}/c^2)^2\ ,$$

which is a circle of radius ≈ 35 MeV around the π^0 mass. The above mass windows are approximately $\pm 3\sigma$ of our expected mass resolution for π^0's and η's.

Events satisfying these requirements are then kinematically fit to $\eta\pi^0\pi^0$ and $\pi^0\pi^0\pi^0$ hypotheses, using only the η and π^0 mass constraints. The fit with the best confidence level is used. An event is kept if the best fit is $\eta\pi^0\pi^0$ and has a confidence level greater than 0.01. The energies and angles from the fit are used for the remainder of this analysis. This improves the $\eta\pi^0\pi^0$ mass resolution at the η' from 25 to 10 MeV, at the expense of a 20% loss in efficiency from cases where a $3\pi^0$ combination gives a better fit.

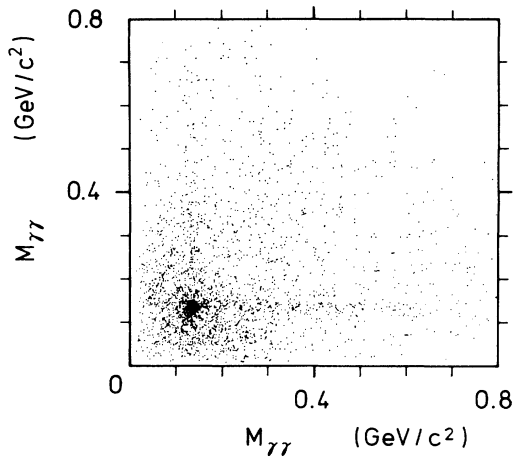

FIG. 4. $M_{\gamma\gamma}$ vs $M_{\gamma\gamma}$ after selecting events with an η. There are three entries per η candidate. An event can have more than one η candidate.

Figure 5 shows the $|\sum \mathbf{p}_t|^2$ distribution for events passing the kinematic fit. Here $|\sum \mathbf{p}_t|$ is calculated from the fitted momentum vectors of the six photons. There is a clear peaking at small $|\sum \mathbf{p}_t|^2$, which is the signature for two-photon events. The width of the peak is consistent with our energy resolution and the expected distribution of the two-photon process. The final cut used in this analysis requires $|\sum \mathbf{p}_t|<100$ MeV/c. We are left with a sample of 247 $\eta\pi^0\pi^0$ events.

The distribution of the mass of the $\eta\pi^0\pi^0$ system (Fig. 6) shows a large peak at the η' mass, with few events outside the η' region. Since we do not make a background subtraction, these latter events cannot be regarded as evidence for $\gamma\gamma\to\eta\pi^0\pi^0$ continuum. A fit to the

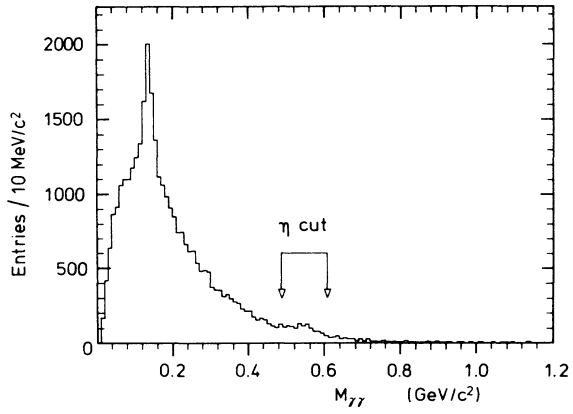

FIG. 3. The $M_{\gamma\gamma}$ distribution for all pairs of photons in six-photon events after a cut $|\sum \mathbf{p}_t|<100$ MeV/c has been applied. Clear peaks at the π^0 and η masses are visible. The arrows indicate the cut at $M_\eta\pm 60$ MeV.

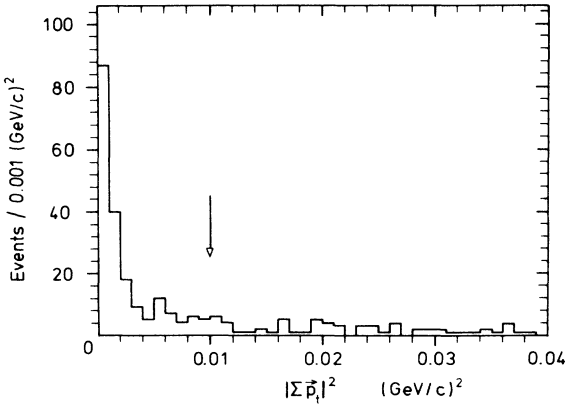

FIG. 5. $|\sum \mathbf{p}_t|^2$ distribution for $\eta\pi^0\pi^0$ events passing the kinematic fit. The arrow indicates the cut at $|\sum \mathbf{p}_t|=100$ MeV/c.

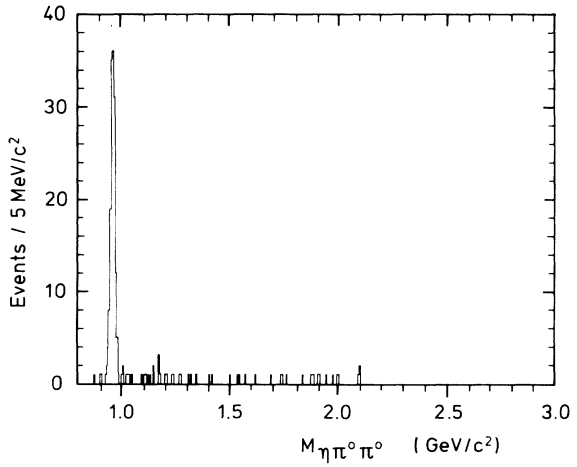

FIG. 6. The $M_{\eta\pi^0\pi^0}$ distribution for the final event sample.

distribution using a Gaussian plus a linear background yields

$$N_{\eta'}=185\pm14 \text{ events} .$$

The fitted mass of 958.9 ± 0.8 MeV is in good agreement with the accepted η' mass,[3] and the fitted width of $\sigma=9.9\pm0.6$ MeV is consistent with Monte Carlo calculations of our resolution for this channel.

IV. DETERMINATION OF $\Gamma_{\eta'\to\gamma\gamma}$

The cross section for production of a narrow pseudoscalar resonance X in no-tag $e^+e^-\to e^+e^-\gamma\gamma$, $\gamma\gamma\to X$ is

$$\sigma_X=8\pi^2\frac{\Gamma_{X\to\gamma\gamma}}{M_X}\times\int\delta[M_X{}^2-(q_1+q_2)^2]\times\frac{2|\mathbf{q}|}{M_X}F^2(q_1)F^2(q_2)\Phi(q_1,q_2)d^4q_1d^4q_2 .$$

The factor in front of the integral is the integrated resonance Breit-Wigner curve for a resonance of spin 0 and mass M_X. The δ function restricts the $\gamma\gamma$ mass to that of the resonance. The q_1 and q_2 are the four-vectors of the two intermediate-state photons; the production rate of such photons is described by $\Phi(q_1,q_2)$. $\Gamma_{X\to\gamma\gamma}$ is conventionally defined to be the partial width to real photons, whereas in the two-photon process the photons are slightly virtual ($q^2<0$). Lorentz and gauge invariance in QED constrain the form of the $\gamma\gamma$-pseudoscalar vertex,[29] leading to the factor $2|\mathbf{q}|M_X$, where $\mathbf{q}$ is the momentum of either photon in the X center of mass. We have used the vector-meson-dominance form factor, $F(q)=1/(1-q^2/m_\rho{}^2)$, with m_ρ the mass of the ρ meson. Our cut of $|\sum\mathbf{p}_t|<100$ MeV effectively restricts our observed data sample to small $|q^2|$, $\langle|q^2|\rangle=(28\text{ MeV})^2$, so that the effect of these form factors on the visible cross section is small.

We use a Monte Carlo event generator based on a program by Vermaseren[4] to calculate $\tilde{\sigma}_{\eta'}$, the above cross section with $\Gamma_{\eta'\to\gamma\gamma}$ set equal to 1 keV. The results were checked with an independent program based on the matrix element given in Ref. 5. Radiative corrections to this process have been shown[6] to be less than 1%.

Then $\Gamma_{\eta'\to\gamma\gamma}$ can be calculated from $N_{\eta'}$ using the following formula:

$$\Gamma_{\eta'\to\gamma\gamma}=\frac{N_{\eta'}}{\mathcal{L}\tilde{\sigma}_{\eta'}\epsilon B_{\eta'\to6\gamma}} .$$

$\mathcal{L}$ is the integrated e^+e^- luminosity and $B_{\eta'\to6\gamma}$ is the branching ratio[7] for $\eta'\to6\gamma$: $B_{\eta'\to6\gamma}\equiv B(\eta'\to\eta\pi^0\pi^0)\times B(\eta\to\gamma\gamma)\times B(\pi^0\to\gamma\gamma)^2=0.086\pm0.008$.

The luminosity was measured from the number N of events which have two and only two energy clusters of energy $>0.7E_{\text{beam}}$ inside $|\cos\theta|<0.75$. The integrated luminosity is then $\mathcal{L}=Ns/c$, where s is the square of the center-of-mass energy. The conversion factor c has been determined from a sample of $e^+e^-(\gamma)$ and $\gamma\gamma(\gamma)$ Monte Carlo events generated with the program of Berends and Kleiss[8] and passed through a detector simulation which uses the EGS electromagnetic shower development code.[9] The systematic error on the luminosity was found to be 2.5%, adding the following in quadrature: 1.0% Monte Carlo statistics, 1.0% for fourth-order QED corrections,[10] 1.9% dependence on the cuts, and 0.2% from hadronic and beam-gas backgrounds.

The efficiency ϵ for an $\eta'\to6\gamma$ event to appear in our final sample is determined from events generated with the Vermaseren Monte Carlo program and passed through the detector simulation. The η' decays according to isotropic phase space; the observed decay distributions agree well with those from the Monte Carlo program.

Some of the selection criteria (in particular the tunnel energy veto) are affected by extra energy deposited in the NaI(Tl) by beam-related backgrounds. This extra energy was measured in a sample of random background events obtained by triggering on ever 10^7th beam crossing, with no other condition. A background event from this sample was added to each η' Monte Carlo event so that efficiences determined from the Monte Carlo program include the effect of this extra energy.

The efficiency of cuts (i)–(iii), the η and π^0 mass cuts, the kinematic fit, and the $|\sum\mathbf{p}_t|$ cut give the constant contribution $\epsilon_{\text{const}}=0.033$ to the overall efficiency.

The trigger efficiency ϵ_{trig} was calculated using the Monte Carlo events which passed the above cuts by subjecting them to the software trigger thresholds described in Sec. III. The results for the various trigger configurations are given in Table II. They do not include the effect of the chamber veto, which is discussed next.

The efficiency for events to pass the chamber veto cut, ϵ_{neut}, is determined by the probability for one of the photons to convert to $\epsilon^+\epsilon^-$ in the beam pipe or in the first two chambers, and by the probability of a noise hit in the third chamber. We determine ϵ_{neut} for each running period by studying $\gamma\gamma\to\pi^0\pi^0$ events in the $f_2(1270)$ region triggered by the 2-hemisphere trigger, which does not have the chamber veto requirement. Cuts similar to those described above (except the chamber cut) result in a sample of 4000 f_2 events, with very small background.

TABLE III. A comparison of our result with published measurements. A dagger indicates that the complete $M1$ matrix element was not used in the $\gamma\rho$ decay; these results are not included in the average.

Experiment	$\Gamma_{\eta'\to\gamma\gamma}$ (keV)	Mode	Reference
Crystal Ball	$4.6\pm0.4\pm0.6$	$\eta\pi^0\pi^0$	This experiment
JADE	4.0 ± 0.9	$\gamma\gamma$	11
TPC/Two-Gamma	$4.5\pm0.3\pm0.7$	$\gamma\rho$	12
TASSO	$5.1\pm0.4\pm0.7$	$\gamma\rho$	13
PLUTO	$3.8\pm0.3\pm0.4$	$\gamma\rho$	14
CELLO†	$(6.2\pm1.1\pm0.8)$	$\gamma\rho$	15
JADE†	$(5.0\pm0.5\pm0.9)$	$\gamma\rho$	16
Mark II	$5.8\pm1.1\pm1.2$	$\gamma\rho$	17
Average	4.3 ± 0.3		

The fraction of these events which do not have the chamber veto bit set is the neutral efficiency for four-photon events, which varied from 81% to 86%, depending on run period. This must then by extrapolated to six-photon events, after taking account of the probability of noise hits, which was measured using the sample of random background events. The resulting values of $\epsilon_{\rm neut}$ are listed in Table II with their statistical errors.

The f_2 sample has also been used to check for effects of variations in the performance of the NaI(Tl) electronics and the data acquisition system during the various running periods. We observe within errors a constant visible f_2 cross section and constant mass and mass resolution of the π^0's.

The overall efficiency is $\epsilon=\epsilon_{\rm const}\times\epsilon_{\rm trig}\times\epsilon_{\rm neut}$. Its average for the whole data sample is 0.022, varying from 0.018 to 0.025. The measured $\Gamma_{\eta'\to\gamma\gamma}\times B_{\eta'\to6\gamma}$ calculated separately for each run period are listed in Table II. The values agree well with each other, and a fit to a constant gives $\chi^2=1.0$ for 5 degrees of freedom. The average is

$$\Gamma_{\eta'\to\gamma\gamma}\times B_{\eta'\to6\gamma}=0.39\pm0.03\pm0.04\ \text{keV}\ ,$$

which gives

$$\Gamma_{\eta'\to\gamma\gamma}=4.6\pm0.4\pm0.6\ \text{keV}\ .$$

Here the first error is statistical and the second is sytematic. The 14% systematic error comes from the following sources (all added in quadrature): uncertainties in the Monte Carlo event generation and detector simulation $\pm5\%$; Monte Carlo statistical error on $\epsilon_{\rm const}\times\epsilon_{\rm trig}\pm3\%$; sensitivity to variations of analysis cuts $\pm5\%$; uncertainties in $\epsilon_{\rm neut}\pm6\%$; uncertainty in the luminosity measurement $\pm2.5\%$; uncertainties in the branching ratios[7] $\eta'\to\eta\pi^0\pi^0$ ($\pm9\%$) and $\eta\to\gamma\gamma$ ($\pm2\%$).

V. DISCUSSION OF THE $\Gamma_{\eta'\to\gamma\gamma}$ RESULT

Our result is compared to published measurements[11–17] of $\Gamma_{\eta'\to\gamma\gamma}$ in Table III. Most previous measurements of the two-photon width of the η' used the decay channel $\eta'\to\gamma\rho$. Since this is a magnetic-dipole transition it affects the angular distribution of the final-state particles. Because of the additional phase-space factor and the large width of the ρ, it also affects the energies of the final-sate particles, with an uncertainty because of the parametrization of the ρ. The JADE and CELLO analyses did not take these effects into account in determining efficiencies. The PLUTO Collaboration state that if they used a phase-space decay matrix element their measurement of $\Gamma_{\gamma\gamma}$ would have been around 5 keV instead of 3.8 keV. The use of the $\eta\pi^0\pi^0$ decay channel avoids these problems, since the η and π^0 are narrow spinless particles. The new world average calculated from our $\eta\pi^0\pi^0$ measurement and those $\gamma\rho$ measurements which used the $M1$ matrix element is 4.3 ± 0.3 keV.

The study of the partial widths of mesons into two photons gives information on their quark content.[18] In order to test whether the π^0, η, and η' mesons can be described in terms of the u, d, and s quarks alone, we interpret our result in the context of the quark model, which yields the following relations for the pseudoscalar nonet:

$$\frac{\Gamma_{\eta\to\gamma\gamma}}{M_\eta{}^3}=\frac{\Gamma_{\pi^0\to\gamma\gamma}}{M_{\pi^0}{}^3}\left[\frac{1}{\sqrt{3}}\cos\theta_P-\frac{\sqrt{8}}{\sqrt{3}}r_P\sin\theta_P\right]^2,$$

$$\frac{\Gamma_{\eta'\to\gamma\gamma}}{M_{\eta'}{}^3}=\frac{\Gamma_{\eta^0\to\gamma\gamma}}{M_{\pi^0}{}^3}\left[\frac{1}{\sqrt{3}}\sin\theta_P+\frac{\sqrt{8}}{\sqrt{3}}r_P\cos\theta_P\right]^2,$$

where θ_P is the SU(3) mixing angle and the r_P is the ratio of the decay constants for the singlet and octet members of the nonet: $r_P=F_8/F_1$. Using $\Gamma_{\pi^0\to\gamma\gamma}=7.5\pm0.5$ eV from Ref. 3 and the average $\Gamma_{\eta\to\gamma\gamma}=0.54\pm0.05$ keV of the published results from two-photon experiments,[11,19,20] together with our value $\Gamma_{\eta'\to\gamma\gamma}=4.6\pm0.7$ keV, we obtain

$$\theta_P=-18.1^\circ\pm2.4^\circ\ ,$$

$$r_P=0.96\pm0.06\ .$$

The result $r_P\approx1$ implies nonet symmetry; i.e., the wave functions at the origin for the octet and singlet states are the same. The value for θ_P is twice as large as that obtained from the quadratic Gell-Mann–Okubo mass formula: $\theta_P(\text{GMO})=-10^\circ$. However, a recent calculation[21] of first-order corrections to both the $\Gamma_{\gamma\gamma}$ and mass formulas shows that although the corrections

to $\Gamma_{\gamma\gamma}$ are small, the corrections to the Gell-Mann–Okubo mass formula can be large, and a consistent picture possible with $\theta_P \approx -20°$. The uncorrected linear Gell-Mann–Okubo mass formula gives $\theta_P = -23°$.

VI. SEARCH FOR OTHER STATES

We have also searched for other states decaying into $\eta\pi^0\pi^0$. Radially excited pseudoscalar mesons are expected[22–24] to be in the 1–2 GeV mass range. Furthermore, a radially excited η or η' is expected to have a substantial branching ratio into $\eta\pi\pi$ (Ref. 23).

As can be seen from Fig. 6, there are very few events in this mass range. We have calculated the 90%-confidence-level (C.L.) upper limit for $\Gamma_{X\to\gamma\gamma}\times B_{X\to\eta\pi\pi}$ as a function of the mass of the resonance X. We have included a factor 3 for $I=0$ to convert the limit on $\eta\pi^0\pi^0$ to $\eta\pi\pi$ (note that an isovector cannot decay into $\eta\pi^0\pi^0$). Our 10% systematic error was conservatively accounted for by multiplying the upper limit by $1+1.28\times 0.10$ (1.28σ corresponds to a 90% C.L. upper limit). The results for total widths of 50 and 200 MeV are shown in Fig. 7. The limit increases with increasing mass because of the decreasing $\gamma\gamma$ flux and detection efficiency.

A candidate for a radially excited pseudoscalar which decays to $\eta\pi\pi$ is the $\eta(1275)$. It has been observed in hadronic collisions by two experiments[25,26] which report total widths of 70 ± 15 and 32 ± 10 MeV, respectively. If the total width is less than 50 MeV, as indicated by the more recent, higher statistics experiments, our 90% C.L. upper limit is

$$\Gamma_{\eta(1275)\to\gamma\gamma}\times B_{\eta(1275)\to\eta\pi\pi} < 0.3 \text{ keV} .$$

Calculations[27,24] for a radially excited pseudodscalar at this mass in models which include the effect of its mixing with the η and η' yield an expected two-photon width of order 2 keV. Thus the $\eta(1275)$ is not described by those mixing models unless it has a small branching ratio to $\eta\pi\pi$.

The experiment of Ref. 26 has also observed a pseudoscalar $\eta\pi\pi$ resonance at 1420 ± 5 MeV with a total of 31 ± 7 MeV. Again assuming the total width is less than 50 MeV, we obtain

$$\Gamma_{\eta(1420)\to\gamma\gamma}\times B_{\eta(1420)\eta\pi\pi} < 0.3 \text{ keV}.$$

A narrow peak at ~ 1390 MeV has been seen in the $\eta\pi\pi$ spectrum from radiative J/ψ decays.[28] If this is a pseudoscalar of width less than 50 MeV, our limit is

$$\Gamma_{X(1390)\to\gamma\gamma}\times B_{X(1390)\to\eta\pi\pi} < 0.27 \text{ keV} .$$

In all three cases the upper limit remains below 0.4 keV if the total width is raised to 100 MeV. Other pseudoscalar candidates as yet unseen may be wider, but even a total width of 200 MeV does not allow $\Gamma_{\gamma\gamma}\times B_{\eta\pi\pi}=2$ keV for masses below 1800 MeV. These results present a challenge to our understanding of the radially excited pseudoscalar nonet.

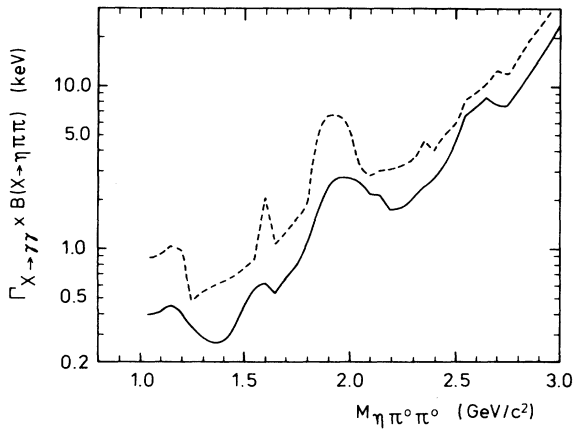

FIG. 7. 90%-confidence-level upper limits for $\Gamma_{X\to\gamma\gamma}\times B_{X\to\eta\pi\pi}$ for a spin-0 resonance X as a function of its mass M_X. The solid line is for total width $\Gamma_X=50$ MeV and the dashed line for $\Gamma_X=200$ MeV.

ACKNOWLEDGMENTS

We would like to thank the DESY and SLAC directorates for their support. This experiment would not have been possible without the dedication of the DORIS machine group as well as the experimental support groups at DESY. Those of us from abroad wish to thank the DESY laboratory for the hospitality extended to us while working at DESY. We acknowledge useful discussions with S. Godfrey, N. Isgur, J. Olsson, and M. Peskin. Z.J., B.N., and G.N. thank DESY for financial support. D.W. acknowledges support from the National Science Foundation. E.D.B., R.H., and K.S. have benefited from financial support from the Humboldt Foundation. S.C. acknowledges support from the Massachusetts Institute of Technology. The Nijmegan group acknowledges the support of Stichting voor Fundamenteel Onderzoek der Materie-Nederlandse Organisatie voor Zviver-Wetenschappelijk Onderzoek (FOM-ZWO). The Erlangen, Hamburg, and Würzburg groups acknowledge financial support from the German Federal Minister for Research and Technology (BMFT) under Contracts Nos. 054 ER 11P(5), 054 HH 11P(7), 054 WU 11P(1) and from the Deutsche Forschungsgemeinschaft (Hamburg). This work was supported in part by the U.S. Department of Energy under Contracts Nos. DE-AC03-81ER40050 (CIT), DE-AC02-76ER03066 (CMU), DE-AC02-76ER03064 (Harvard), DE-AC02-76ER03072 (Princeton), DE-AC03-76SF00515 (SLAC), DE-AC03-76SF00326 (Stanford), and by the National Science Foundation under Grants Nos. PHY75-22980 (CIT), PHY81-07396 (HEPL), and PHY82-08761 (Princeton).

[a]Present affiliation: Institute for Particle Physics, University of California, Santa Cruz, CA 95064.
[b]Present affiliation: Massachusetts Institute of Technology, Cambridge, MA 02139.
[c]Present affiliation: Universität München, München, West Germany.
[d]Permanent address: Department de Physique des Particules Elémentaires, Centre d'Etudes Nucléaires de Saclay, Gif-sur-Yvette, France.
[e]Present affiliation: University of Amsterdam, The Netherlands.
[f]Present affiliation: KEK National Laboratory for High Energy Physics, Tsukuba, Japan.
[g]Permanent address: Cracow Institute of Nuclear Physics, Cracow, Poland.
[h]Present affiliation: Vanderbilt University, Nashville, TN 37203.
[i]Present affiliation: Nuclear Physics Laboratory, Oxford University, Keble Road OX1 3RH London, England.
[j]Present affiliation: Lawrence Berkeley Laboratory, Berkeley, CA 94720.
[k]Present affiliation: Fermilab, Batavia, IL 60510.
[l]Present affiliation: III. A Physikalisches Institut, Rheinisch-Westfälishe Technishe Hochschule Aachen, Aachen, West Germany.
[m]Present affiliation: CERN/EP, Geneva, Switzerland.

[1]E. D. Bloom and C. W. Peck, Annu. Rev. Nucl. Part. Sci. **33**, 143 (1983); M. Oreglia *et al.*, Phys. Rev. D **25**, 2259 (1982).

[2]The measured energy $E_{\rm meas}$ of each photon has been corrected using the formula $E_{\rm corr}=E_{\rm meas}/[1+0.0137\ln(E_{\rm meas}/E_{\rm beam})]$. The use of this formula correctly game the π^2 mass and mass difference $M_{\Upsilon(2S)}-M_{\Upsilon(1S)}$ in the reaction $\Upsilon(2S)\to\pi^0\pi^0\Upsilon(1S)$, which were otherwise $\approx 5\%$ too low. This downward shift stems from the extrapolation of the calibration energy (5 GeV from Bhabha events) down to the energy range of 20–300 MeV. A discussion of this effect, and derivation of the form of the correction can be found in D. Gelphman, Ph.D. thesis, Stanford, Report No. SLAC-286, 1985.

[3]Particle Data Group, M. Aguilar-Benitez *et al.*, Phys. Lett. **170B**, 1 (1986).

[4]J. A. M. Vermaseren, Nucl. Phys. **B229**, 347 (1983).

[5]G. Bonneau, M. Gourdin, and F. Martin, Nucl. Phys. **B54**, 573 (1973).

[6]M. Defrise *et al.*, Phys. Rev. D **23**, 663 (1981).

[7]We used $B(\eta'\to\eta\pi^0\pi^0)=0.23\pm0.02$ given on p. 182 of Ref. 3 rather than rely on isospin to calculate it from the better measured $B(\eta'\to\eta\pi^+\pi^-)$.

[8]F. A. Berends and R. Kleiss, Nucl. Phys. **B228**, 537 (1983); **B186**, 22 (1981).

[9]R. Ford and W. Nelson, Report No. SLAC-210, 1978 (unpublished).

[10]B. Naroska, Phys. Rep. **148**, 98 (1987).

[11]JADE Collaboration, W. Bartel *et al.*, Phys. Lett. **160B**, 421 (1985). The error on $\Gamma_{\eta'\to\gamma\gamma}$ is statistical only and dominates over the systematic error [J. Olsson (private communication)].

[12]TPC/Two-Gamma Collaboration, H. Aihara *et al.*, Phys. Rev. D **35**, 2650 (1987).

[13]TASSO Collaboration, M. Althoff *et al.*, Phys. Lett. **147B**, 487 (1984).

[14]PLUTO Collaboration, Ch. Berger *et al.*, Phys. Lett. **142B**, 125 (1984).

[15]CELLO Collaboration, H. J. Behrend *et al.*, Phys. Lett. **114B**, 378 (1982); **125B**, 518(E) (1983).

[16]JADE Collaboration, W. Bartel *et al.*, Phys. Lett. **113B**, 190 (1982).

[17]Mark II Collaboration, G. S. Abrams *et al.*, Phys. Rev. Lett. **43**, 477 (1979); P. Jenni *et al.*, Phys. Rev. D **27**, 1031 (1983). Although it is not explicitly stated in the papers, the $M1$ matrix element was used [V. Telnov (private communication)].

[18]S. Matsuda and S. Oneda, Phys. Rev. **187**, 2107 (1969); S. Okubo, in *Symmetries and Quark Models,* edited by R. Chand (Gordon and Breach, New York, 1970), p. 59; H. Suura *et al.*, Lett. Nuovo Cimento **4**, 505 (1972); A. Bramon *et al.*, Phys. Lett. **48B**, 137 (1974); F. Gault *et al.*, Nuovo Cimento **24A**, 259 (1974); M. Chanowitz, Phys. Rev. Lett. **35**, 977 (1975); E. Etim *et al.*, Nuovo Cimento **43**, 124 (1977); N. M. Chase *et al.*, Z. Phys. C **2**, 23 (1979); M. Chanowitz, Phys. Rev. Lett. **44**, 59 (1980); J. L. Rosner, Phys. Rev. D **27**, 1101 (1983).

[19]Crystal Ball Collaboration, A. Weinstein *et al.*, Phys. Rev. D **28**, 2896 (1983).

[20]TPC/Two-Gamma Collaboration, H. Aihara *et al.*, Phys. Rev. D **33**, 844 (1986).

[21]J. F. Donoghue, B. R. Holstein, and Y.-C. R. Lin, Phys. Rev. Lett. **55**, 2766 (1985); see, also, G. Grunberg, Phys. Lett. **168B**, 141 (1986).

[22]R. H. Graham and P. J. O'Donnell, Phys. Rev. D **19**, 284 (1979).

[23]I. Cohen and H. J. Lipkin, Nucl. Phys. **B151**, 16 (1979).

[24]S. Godfrey and N. Isgur, Phys. Rev. D **32**, 189 (1985).

[25]N. R. Stanton *et al.*, Phys. Rev. Lett. **42**, 346 (1979).

[26]A. Ando *et al.*, Phys. Rev. Lett. **57**, 1296 (1986).

[27]M. Frank and P. J. O'Donnell, Phys. Rev. D **32**, 1739 (1985).

[28]Mark III Collaboration, L. Köpke in *Proceedings of the XXIII International Conference on High Energy Physics,* Berkeley, California, 1986, edited by S. Loken (World Scientific, Singapore, 1987); (DM2) Collaboration, B. Jean-Marie, *ibid.*

[29]G. Köpp, T. F. Walsh, and P. Zerwas, Nucl. Phys. **B70**, 461 (1974).